Electronic Supplementary Material (ESI) for Journal of Materials Chemistry A.

Supplementary Information

Cassie-Baxter State Stability of a 3D Micro-nano Hierarchical Superhydrophobic Surface Fabricated by a Laser-Chemical Hybrid Method

*Rui Pan, Mingyong Cai, Weijian Liu, Xiao Luo, Changhao Chen, Hongjun Zhang, Minlin Zhong**

Laser Materials Processing Research Center, School of materials science and engineering, Tsinghua University, Beijing, P. R. China, 100084

*Email: zhml@tsinghua.edu.cn

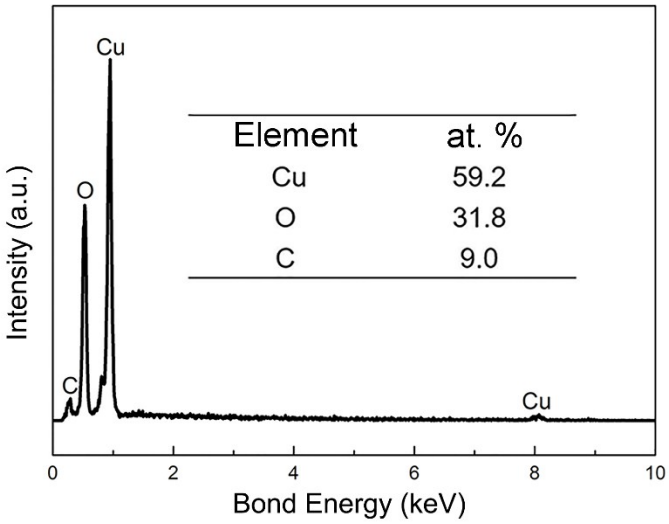

Figure S1. EDS analysis of the marked area A in Fig. 1(f1)

Table S1. The fabrication conditions and structural parameters of different MNT structures

Samples	Laser ablation		Chemical oxidation		Microcones		Nanorods
	Interval (μm)	Time	Temperature	Time (min)	Periodity (μm)	Height (μm)	Length (μm)
P40	40	35	RT	20	40±2	50±3	15±2
P60	60	35	RT	20	60±2	50±3	15±2
P80	80	35	RT	20	80±3	50±3	15±2
H15	40	10	RT	20	40±2	15±2	15±2
H30	40	25	RT	20	40±2	30±2	15±2
L5	40	35	RT	5	40±2	50±3	5±1
L10	40	35	RT	10	40±2	50±3	10±2

Tape peeling tests:

As can be seen in Fig. S2, with the increase of tapping cycles, CA decreases and SA increases gradually. But the CA keeps larger than 150° and SA stays less than 10° even after 500 tapping cycles, indicating a good bonding strength between the fluoroalkyl silane layer and the micro-nanostructures.

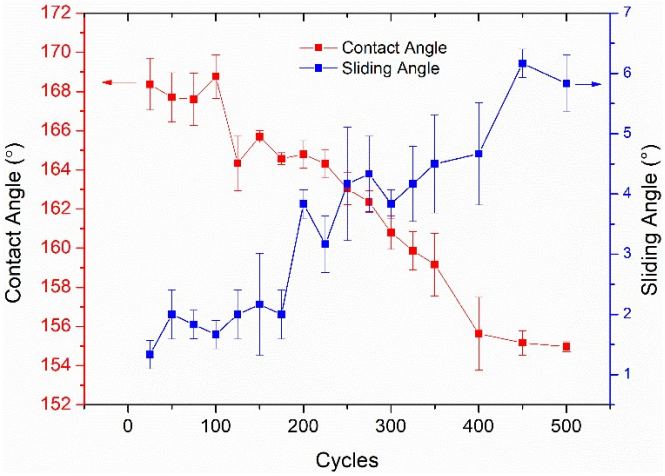

Figure S2 Dependence of contact and sliding angles vs. tapping cycles

Table S2. P_{CCA}, P_{CTD} and P_{CCB} of different MNR surfaces with different structural parameters and whether Wenzel state occurs or not (All the measured/calculated numerical values are averages. The uncertainties can be found in *Methods Section.*)

Periodicity (μm)	Height (μm)	Nanorod length (μm)	Laplace Pressures (Pa)			Wenzel state
			P_{CCA}	P_{CTD}	P_{CCB}	
40	50	15	1100	845	845	Yes
60	50	15	900	600	600	Yes
80	50	15	678	400	400	Yes
40	15	15	912	860	860	Yes
40	30	15	1030	886	886	Yes
40	50	5	370	560	370	No
40	50	10	670	700	670	No

Table S3. P_{CCA}, P_{CTD} and P_{CCB} of different hierarchical surfaces and whether Wenzel state occurs or not (All the measured/calculated numerical values are averages. The uncertainties can be found in *Methods Section.*)

Surfaces	Different Critical Laplace Pressure (Pa)			Wenzel state
	P_{CCA}	P_{CTD}	P_{CCB}	
SM	220	619	220	No
SN	530	682	530	No
MNW	470	675	470	No
MNG	615	824	615	No
MNR	1100	844	844	YES
Triple-scale	1450	1450	1450	No

Calculation of CA equations for different wetting states:

In the calculation, a periodic structural unit cell with a dual-scale roughness, composed of parabolic microcone pattern covered with uniformly distributed nano-rods was considered. To avoid a mathematical instability beyond the existence of a local minimum[S1] and the case that the projected area of the solid surface wetted by the liquid equals to zero, a circular flat domain (top platform) on the top of the microcone pattern was assumed, as sketched in Fig. 8(a). The following additional assumptions are considered in the calculations: (i) the shape of the water droplet is hemispherical, and the solid-liquid contact line is circular; (ii) the water droplet size is much larger than the structural unit cell and the structural size is smaller than capillary length, so gravity and line tension are negligible; (iii) the volume of water penetrated in the roughness features of the substrate surface is negligible vs. the volume of the droplet. The system domain Ω considered includes all the interfaces of the droplet, the whole textured solid surface (i.e., not only the area covered with the droplet but also the area not covered with the droplet) and the air trapped in the rough surface features.

Thus, the free energy of the system Ω can be written as the following expression:

$$G = A_{lg} \cdot \sigma_{lg} + A_{ls} \cdot \sigma_{ls+} A_{sg} \cdot \sigma_{sg} \quad \text{(S1)}$$

In Eq. (S1), A_{lg}, A_{ls} and A_{sg} are the areas of liquid-gas, liquid-solid, and solid-gas interfaces, respectively. σ_{lg}, σ_{ls} and σ_{sg} are the specific surface free energies of liquid-gas, liquid-solid, and solid-gas interfaces, respectively.

The structural parameters subscripted *1*, *2* and *top* shown in Fig. 8(a) and (b) denote the structures of nanorods, microcones and the platform on the top of the microcone, respectively. f_i and r_i (*i=1*, *2* and *top*, respectively) denote the surface fraction and roughness factor (the ratio of the real surface area to the planar surface

area) of the corresponding structures. a_1, and h_1 are the hip diameter and height of the microcones. D_2 and h_2 are the diameter and height of nanorods. b_1 and b_2 denote the interval between two microcones and two nanorods, respectively. The radius of the top platform is assumed to be a_1/k (k>1, denotes the proportion of the top platform diameter to the hip diameter of the microcones.). All the structural parameters are schematically shown in Fig. 8(a) and (b).

For CB-CB:

$$\cos\theta^{CB}_{E}{}^{-CB} = f_2 \cdot f_{top} \cdot cos\theta_0 + f_2 \cdot f_{top} - 1 \tag{S2}$$

in which, θ_0 is the intrinsic CA of copper after fluoroalkyl silane chemical modification.

For CB-W:

$$\cos\theta^{CB}_{E}{}^{-W} = r_2 \cdot r_1 \cdot cos\theta_0 \tag{S3}$$

For W-CB:

$$\cos\theta^{W}_{E}{}^{-CB} = f_2 \cdot r_1 \cdot cos\theta_0 - {r_1}^* \tag{S4}$$

For W-W:

$$\cos\theta^{W}_{E}{}^{-W} = r_2 \cdot f_{top} \cdot cos\theta_0 + f_{top} - 1 \tag{S5}$$

In above equations,

$$f_{top} = \pi(a_1/k)^2/(a_1 + b_1)^2$$

$$r_2 = 1 + 4 \cdot f_2 \cdot h_2/D_2$$

$$r_1 = \left[S_1 + \pi(a_1/k)^2 - \pi {a_1}^2\right]/(a_1 + b_1)^2 - 1$$

$${r_1}^* = \frac{(S_2 - S_1 \cdot f_2) + \pi(1 - f_2) \cdot \left[(a_1/k)^2 - \left(a_1 + h_2 \cdot \sin\theta^*\right)^2\right]}{(a_1 + b_1)^2} + 1 - f_2$$

where

$$S_1 = \int_{\frac{a_1}{k}}^{a_1} 2x\pi\sqrt{1 + {y_1}'^2}dx$$

$$S_2 = \int_{\frac{a_1}{k}}^{a_1 + h_2 \cdot \sin\theta^*} 2x\pi\sqrt{1 + y_2^{'2}}dx$$

in which y_1 and y_2 are the curve profile equations of the microcone and the outside edge of the nanorods normally grown along the microcone, respectively, as shown in Fig. 8(a):

$$y_1 = -h_1/a_1^2 \cdot x^2 + h_1$$

$$y_2 = -\left(h_1 + h_2 - h_2 \cdot \cos\theta^*\right)/\left(a_1 + h_2 \cdot \sin\theta^*\right)^2 \cdot x^2 + h_1 + h_2$$

Following minimization of free energy, the G for different wetting states can be written in a form as follows:

$$G = A_{ext} \cdot \sigma_{lg} + A_{total} \cdot r_1 \cdot r_2 \cdot \sigma_{sg} - cos\theta_E \cdot A_{base} \cdot \sigma_{lg} \quad \text{(S6)}$$

In Eq. (S6), $A_{ext} = 2\pi R^2(1 - cos\theta)$, $A_{base} = \pi R^2(1 - cos^2\theta)$. θ_E^i is the corresponding CA of the equilibrium wetting state i (i=CB-CB, CB-W, W-CB and W-W, respectively.).

Then, the normalized free energy G^* can be expressed as[S2]:

$$G^* = \frac{G - \sigma_{sg} \cdot r_1 \cdot r_2 \cdot S_{total}}{\sigma_{lg}} = \frac{2(1 - \cos\theta) - \cos\theta_E^i \cdot sin^2\theta}{(2 - 3\cos\theta + cos^3\theta)^{2/3}} = \frac{2(1 - \cos\theta) - \cos\theta_E^i \cdot sin^2\theta}{((cos\theta - 1)^2(cos\theta + 2))^{2/3}} \quad \text{(S7)}$$

The first derivative of G versus $cos\theta$ *is:*

$$\frac{\partial G^*}{\partial cos\theta} = \frac{\left(cos\theta - cos\theta_E^i\right)(cos\theta + 1)^2}{\left[(cos\theta - 1)^2(cos\theta + 2)\right]^{5/3}} \quad \text{(S8)}$$

It can be seen from Eq. (S8) that the minimum free energy will be obtained at θ=*180*°, ($cos\theta$ = -1) or $cos\theta = cos^{\theta_E^i}$ when $\frac{\partial G^*}{\partial cos\theta} = 0$. Since θ=*180*° doesn't correspond to a real case of a droplet sitting on a solid surface, the minimum free energy can only be taken when $cos\theta = cos\theta_E$.

Reference:

S1 A. Marmur, Langmuir, 2003, 19, 8343-8348.

S2 H. Wu, K. Zhu, B. Wu, J. Lou, Z. Zhang and G. Chai, Appl. Surf. Sci., 2016, 382, 111-120.

Monotonicity Analysis of The Normalized Free Energy G^*

According to Eq. (S7), when $\theta=\theta_E^i$, the normalized free energy can be written as follows:

$$G^* = (2 - 3\cos\theta + cos^3\theta)^{1/3} \quad \text{(S9)}$$

Then the first derivative of G^*versus $cos\theta$ is:

$$\frac{dG^*}{dcos\theta} = \frac{cos^2\theta - 1}{(2 - 3\cos\theta + cos^3\theta)^{2/3}} = \frac{cos^2\theta - 1}{((cos\theta - 1)^2(cos\theta + 2))^{2/3}} \quad \text{(S10)}$$

Since -1<cosθ<1 (0<θ<180°) and 0<$cos^2\theta$<1, it is easy to see that $\frac{dG^*}{dcos\theta}$<0, indicating that G^* is monotonically decreasing with $cos\theta$. However, $cos\theta$ is monotonically decreasing with θ (0<θ<180°), thus G^* is monotonically increasing with θ.

Table S4. Comparison of critical Laplace Pressure[1] of the two and triple-scale hierarchical micro-nano structures fabricated in present study with several typical previous reports

References	Metal	Structures	Fabrication method	Laplace Pressure (Pa)	Year
28	Silicon	Single-scale: micropillars	Chemical Vapor Deposition	200Pa	2019
23	Cu	Two-scale: Microcones with nanoparticles	Ultrafast Laser	400 Pa	2016
27	PDMS	Single-scale: micropillars	photolithography	<200Pa	2016
30	copper	Mushroom-like structure	photolithography and electroplating	<800Pa	2015
46	PDMS	Single-scale: Micropillars	lithography	<700Pa	2013
31	Silica	Single-scale: micropillars	Sol-gel +Lithography	<300Pa	2013
35	Silicon	Two-scale: Micro and nano-sheets	Two steps of Thermal Deposition	<300Pa	2013
32	PDMS	Single-scale: Micropillars	--	<300Pa	2011
29	PDMS	Single-scale: Micropillars	micromolding	~500 Pa	2010
47	Silicon	Single scale: sharp-tip nanoposts	Lithography+ Reactive Ion Etching	500 Pa	2009
48	silicon	Single-scale: Micropillars	Photolithography	<300 Pa	2007
49	PDMS silicon elastomer	Single-scale: Micropillars	Soft-Lithography	<450 Pa	2006
This research	Cu	Two-scale: Microcones with nanorods	Ultrafast Laser+Chemical	845 Pa	--
This research	Cu	Three-scale: Microcones with nanosheets and micro-balls	Ultrafast Laser+Chemical	1450 Pa	--

[1] The critical Laplace pressure in others' studies are actually the critical Laplace pressure P_{CCA}, denoting the transition from superhydrophobic to hydrophobic state; while the critical Laplace pressure in present study is the critical Laplace pressure P_{CCB}, which can comprehensively indicate the critical moment that a droplet loses its CB state on a superhydrophobic surface.

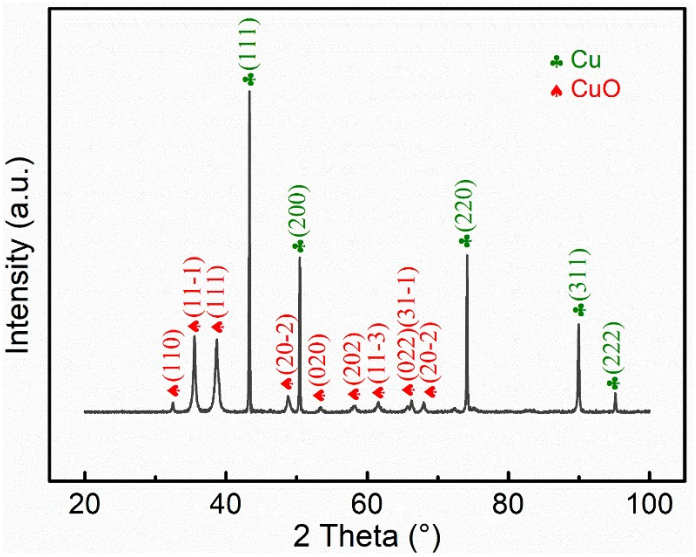

Figure S3. XRD analysis of the prepared superhydrophobic surface with triple-scale structures

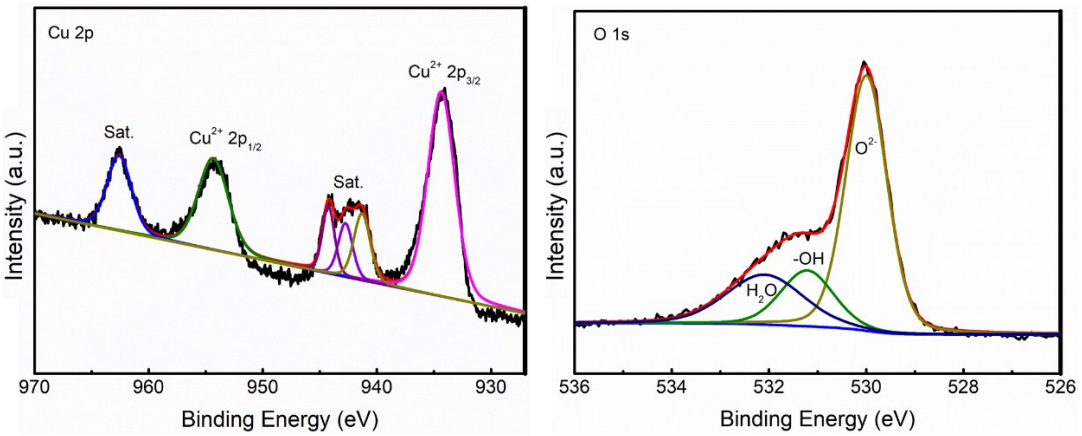

Figure S4 XPS analysis of the prepared superhydrophobic surface with triple-scale structures

Calculation Method of the Laplace Pressure:

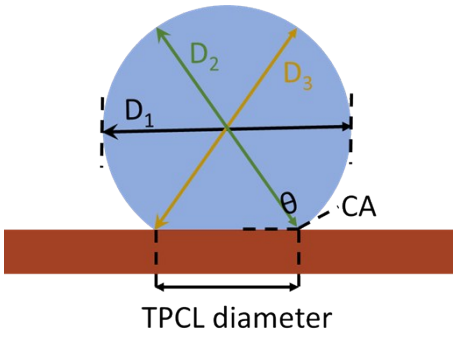

Figure S5. The schematic of a droplet sitting on a superhydrophobic surface

Laplace pressure P in present study is calculated by the following equation:

$$P = \frac{2\gamma}{R} = \frac{2\gamma}{\left((1/3)\left(1/2\sum_{1}^{3} D\right)\right)} = \frac{12\gamma}{D_1 + D_2 + D_3} \quad \text{(S11)}$$

in which, γ is the surface tension of water; R is the averaged radius of the water droplet; D_1, D_2 and D_3 are illustrated in Fig. S3.